Journal Pre-proof

An insight into the synthesis of cationic porphyrin-imidazole derivatives and their photodynamic inactivation efficiency against *Escherichia coli*

Xavier Moreira, Patrícia Santos, M. Amparo F. Faustino, M. Manuela M. Raposo, Susana P.G. Costa, Nuno M.M. Moura, Ana T.P.C. Gomes, Adelaide Almeida, M.G.P.M.S. Neves

Please cite this article as: Moreira X, Santos Patrí, Faustino MAF, Raposo MMM, Costa SPG, Moura NMM, Gomes ATPC, Almeida A, Neves MGPMS, An insight into the synthesis of cationic porphyrin-imidazole derivatives and their photodynamic inactivation efficiency against *Escherichia coli*, *Dyes and Pigments* (2020), doi: https://doi.org/10.1016/j.dyepig.2020.108330.

This is a PDF file of an article that has undergone enhancements after acceptance, such as the addition of a cover page and metadata, and formatting for readability, but it is not yet the definitive version of record. This version will undergo additional copyediting, typesetting and review before it is published in its final form, but we are providing this version to give early visibility of the article. Please note that, during the production process, errors may be discovered which could affect the content, and all legal disclaimers that apply to the journal pertain.

An insight into the synthesis of cationic porphyrin-imidazole derivatives and their photodynamic inactivation efficiency against *Escherichia coli*

Xavier Moreira,[a] Patrícia Santos,[b] M. Amparo F. Faustino,[a] M. Manuela M. Raposo,[c] Susana P. G. Costa,[c] Nuno M. M. Moura,[a,*] Ana T. P. C. Gomes,[b,*] Adelaide Almeida,[b] M. G. P. M. S. Neves[a,*]

[a] *LAQV-REQUIMTE, Department of Chemistry, University of Aveiro, 3810-193 Aveiro, Portugal. E-mail: nmoura@ua.pt; gneves@ua.pt*

[b] *CESAM and Department of Biology, University of Aveiro, 3810-193 Aveiro, Portugal. E-mail: ana.peixoto@ua.pt;*

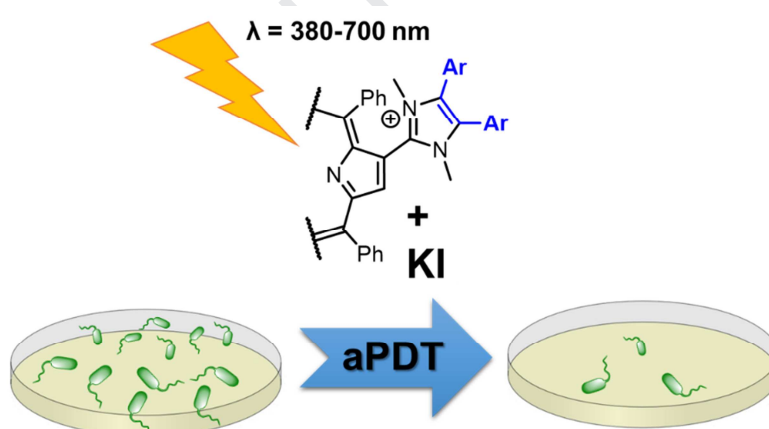[c] *Centro de Química, Universidade do Minho, Campus de Gualtar, 4710-057 Braga, Portugal.*

An insight into the synthesis of cationic porphyrin-imidazole derivatives and their photodynamic inactivation efficiency against *Escherichia coli*

Xavier Moreira,[a] Patrícia Santos,[b] M. Amparo F. Faustino,[a] M. Manuela M. Raposo,[c] Susana P. G. Costa,[c] Nuno M. M. Moura,[a,*] Ana T. P. C. Gomes,[b,*] Adelaide Almeida,[b] M. G. P. M. S. Neves[a,*]

[a] LAQV-REQUIMTE, Department of Chemistry, University of Aveiro, 3810-193 Aveiro, Portugal. E-mail: nmoura@ua.pt; gneves@ua.pt

[b] CESAM and Department of Biology, University of Aveiro, 3810-193 Aveiro, Portugal. E-mail: ana.peixoto@ua.pt;

[c] Centro de Química, Universidade do Minho, Campus de Gualtar, 4710-057 Braga, Portugal.

Abstract

New porphyrin-imidazole derivatives were synthesized by Radziszewski reaction between 2-formyl-5,10,15,20-tetraphenylporphyrin **1** and several (hetero)aromatic 1,2-diones, which after cationization afforded promising monocationic photosensitizers **3a-d**. Singlet oxygen studies have demonstrated that all the cationic porphyrin-imidazole conjugates **3a–d** were capable to produce cytotoxic species. These photosensitisers were able to photoinactivate *Eschericha coli* and their inactivation profile was improved in the presence of KI.

1. Introduction

In the last years, antimicrobial resistance to antibiotics has been intensified and it is considered a global threat to human health. Infections caused by resistant bacteria which may not be treated with antibiotics, are a major warning to public health, with an increased risk of morbidity and mortality, and consequently increasing the healthcare costs.[1, 2] The spread of drug resistant bacteria and the lack of adequate antibiotics, requires the urgently development of new and effective alternative therapies to antibiotics.

Antimicrobial Photodynamic Therapy (aPDT) is reported in the literature as a promising alternative to antibiotic treatment; in this therapeutic approach the combined action of a photosensitizer (PS), light and molecular oxygen induces the production of

reactive oxygen species (ROS), such as singlet oxygen ($^1O_2$), triggering microbial inactivation.[3, 4] aPDT is a multitarget therapy, acting mainly on the outer structures, affecting also nucleic acids. [3, 5] Consequently, the development of resistance to this therapy is highly improbable.[4, 6, 7] aPDT has already proved its efficiency against Gram-positive and Gram-negative bacteria, viruses, fungi and other parasites.[8, 9]

Among the PSs studied within the photoinactivation of microorganisms by aPDT, porphyrins are, indubitably, the foremost considered class of compounds. Nowadays, several research groups are focused in the development of new synthetic approaches for providing porphyrin derivatives with proper features for their application in aPDT.[10-12] One of the strategies used consists of coupling different moieties with recognized and well-established pharmacological activities. In this context, porphyrins can be linked to other biologically active molecules, aiming to increase their biological efficacy.[10, 13] Having in mind the already known photodynamic effect of porphyrins and the antimicrobial, fungicidal and cytotoxic activity of imidazoles,[14] as well as their interesting optoelectronic properties giving rise to a wide range of applications (*e.g.* optical chemosensors and nonlinear optical (SHG, TPA) chromophores),[15-17] in this work we reported the synthesis and the photodynamic activity of novel cationic porphyrin-imidazole derivatives by coupling of 2-formyl-5,10,15,20-tetraphenylporphyrin **1** to several 1,2-diones under Radziszewski conditions [14] followed by cationization. The synthesis of other porphyrin/imidazole conjugates has been already reported by our group and proved to be efficient in the photoinactivation of *Escherichia coli*. [18] As far as we know, most of the functionalizations of the porphyrinic macrocycle with imidazole rings were performed at the *meso* positions or by axial coordination of the imidazole ring to a metal ion at the porphyrin core.[19-25] In fact, beyond our work only Nath´s group reported the preparation of porphyrin-imidazole derivatives by condensation of diamines with the Ni(II) complex of 2-formyl-porphyrin **1**.[18, 26]

The potentiation of aPDT efficiency with these cationic porphyrin-imidazole derivatives by potassium iodide was also accessed.[27] The KI reacts with $^1O_2$, affording free iodine (I_2/I_3^-), hydrogen peroxide (H_2O_2) and iodine radicals ($I_2^{\cdot-}$), that are extremely bactericidal.[27-34] In fact, several *in vitro* and *in vivo* studies have shown the potentiation of porphyrins, fullerenes, rose bengal and methylene blue by KI towards several microorganisms such as *E. coli*, *Acinetobacter baumannii*, *P. aeruginosa*, C*. albicans* and methicillin-resistant *S. aureus*.[27-29, 32, 35]

2. Results and Discussion

2.1 Synthesis and photophysical properties of porphyrin-imidazole derivatives

The synthetic route to access the mono-cationic porphyrin derivatives **3a-d** required the preparation of the correspondent neutral derivatives **2a-d** as outlined in scheme 1. These intermediates were obtained from 2-formyl-5,10,15,20-tetraphenylporphyrin **1** using the Radziszewski reaction methodology [14]. The (hetero)aromatic diones selected were 1,2-diphenylethane-1,2-dione (**Da**), 1,2-di(pyridin-2-yl)ethane-1,2-dione (**Db**), 1,2-di(furan-2-yl)ethane-1,2-dione (**Dc**) and phenanthrene-9,10-dione (**Dd**).
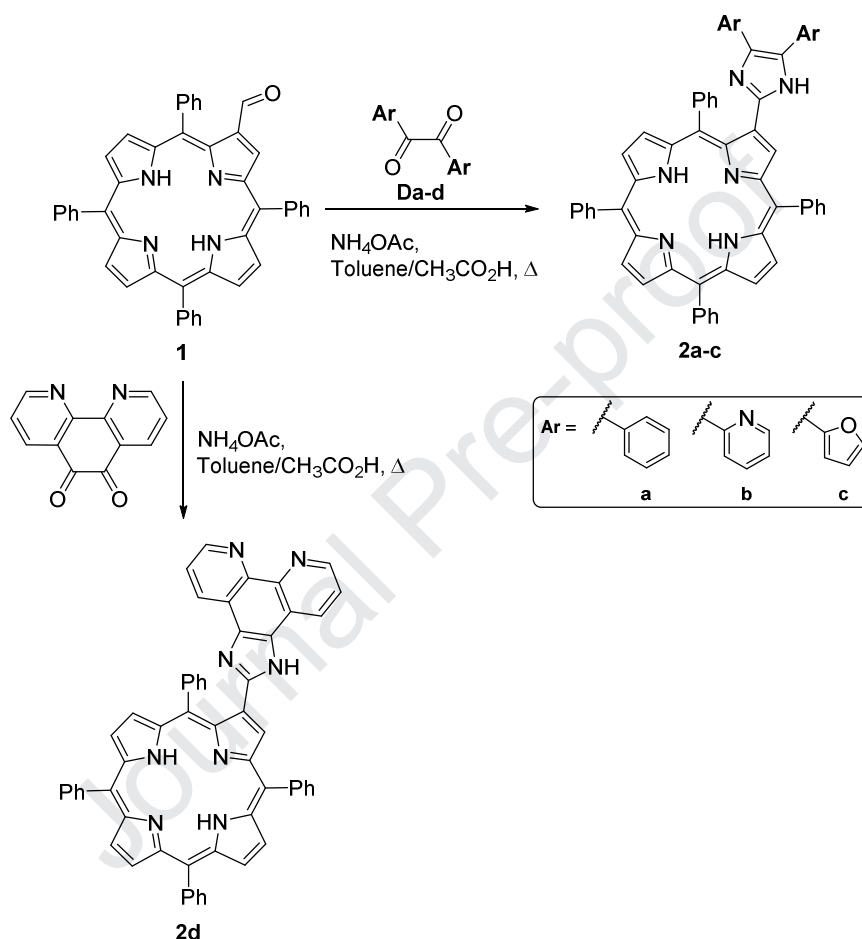

Scheme 1. Radziszewski reaction between 2-formyl-5,10,15,20-tetraphenylporphyrin **1** and a series of 1,2-diones.

The condensation between the 2-formyl-tetraphenylporphyrin **1** and the 1,2-diones selected was performed in the presence of ammonium acetate in a refluxing mixture of toluene/acetic acid (5:1) and stopped when the TLC control showed the full consumption of the starting material **1** (between 1 and 3 hours)**.** After workup and purification by column chromatography, the corresponding porphyrin-imidazole derivatives **2a-d** were isolated in excellent yields, ranging from 79 to 99 % (Table 1).

Table 1. Yields of compounds **2a-d** obtained from the Radziszewski reaction between 2-formyl-tetraphenylporphyrin **1** and a series of 1,2-diones **Da-d**.

Entry	Compound	Time (h)	Yield (%)
1	**2a**	3	79
2	**2b**	3	84
3	**2c**	1	88
4	**2d**	2	99

The cationization of the imidazole moiety of derivatives **2a-d** was performed in the presence of an excess of methyl iodide in *N*,*N*´-dimethylformamide (DMF) for 24 h at 40 ºC as outlined in Scheme 2. After workup, a TLC monitorization confirmed the conversion of all the starting porphyrin-imidazole derivatives **2a-d** into more polar compounds. These new derivatives were identified as the mono-cationic products **3a-d** and were obtained pure in excellent yields (81-97%), directly from crystallization in CH₂Cl₂/hexane.
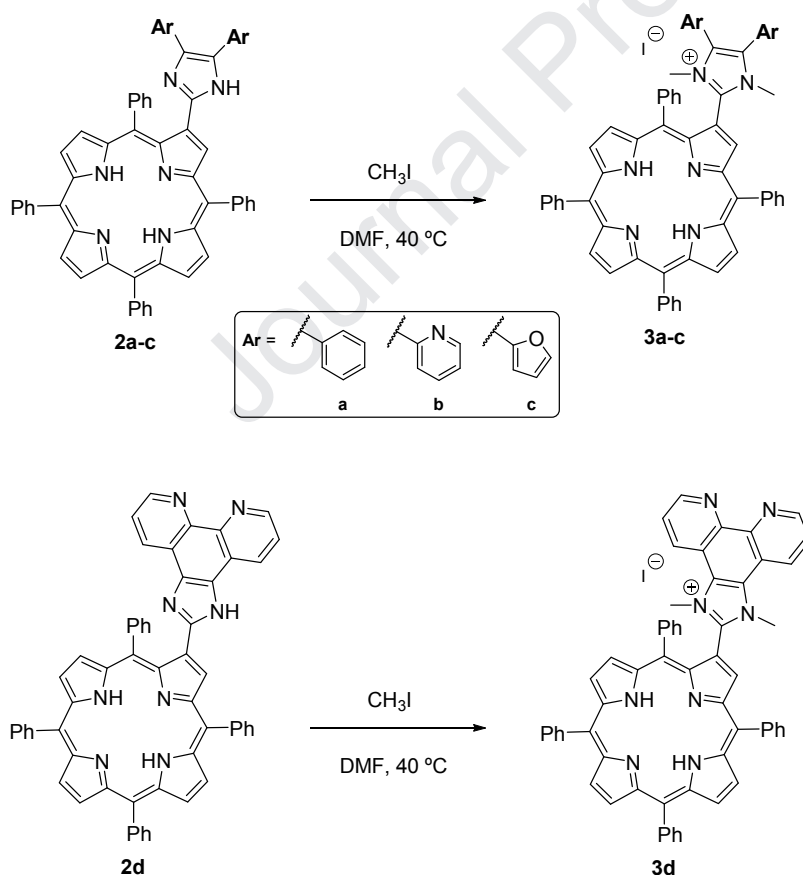
Scheme 2. Alkylation/cationization reaction of compounds **2a-d**.

It is worth to refer that when the cationization/alkylation of compounds **2b** and **2d** was performed, only the mono-cationic derivatives and no products from the additional quaternization of the nitrogens from the pyridine and phenanthroline units were detected.

The structures of both neutral and cationic porphyrin-imidazole conjugates prepared were elucidated by NMR, involving 1D (^{1}H and ^{13}C) and 2D (^{1}H/^{1}H COSY) spectra, HRMS and UV-Vis spectroscopy techniques. The ^{1}H NMR spectra of the neutral derivatives **2a-d** clearly shows the formation of the imidazole ring and are consistent with β-substituted porphyrins, showing a prominent singlet in the range from 13.35 ppm to 12.25 ppm due to the resonance of the *N*-H proton from the imidazole ring and the resonance of the corresponding H-3 as a singlet at *ca.* 9.2 ppm or under the multiplet at *ca.* 8.9 ppm due to the resonances of the other β-pyrrolic protons. The resonances of the protons from the *meso*-phenyl groups arise between *ca.* 8.3 ppm and *ca.* 7.7 ppm and the *meta* and *para* protons of one of the phenyl rings are protected by the presence of the new imidazole core and the signals of their resonances ranging from 7.26 ppm and *ca.* 6.60 ppm.

The most relevant features of the ^{1}H NMR of the mono-cationic derivatives **2a-d** are the absence of the signal due to the resonance of the imidazole N-*H* proton and the appearance of a new singlet in the aliphatic region ranging from 3.82 ppm and *ca.* 3.12 ppm due to the resonances of the protons from the methyl groups.

In both neutral (**2a-d**) and cationic derivatives (**3a-d**), the ^{1}H NMR presents the typical singlet at *ca.* -2.70 ppm generated by the resonances of the *N*-H protons at the porphyrinic inner core, confirming their *free-base* form.

The analysis of the HRMS-ESI(+) spectra shows the presence of a peak with *m/z* corresponding to the [M+H]$^+$ and [M]$^+$ ions, for the neutral derivatives (**2a-d**) and mono-cationic derivatives (**3a-d**), respectively.

The electronic spectra of the neutral and mono-cationic derivatives were recorded and the ability of the cationic derivatives to produce singlet oxygen was measured. For a better evaluation of the influence of the different substituents in the photophysical parameters, all the studies were performed in the same solvent, namely DMF.

Figure 1 shows the absorption spectra of compound **2a** in DMF solutions at a concentration of 3.0 x 10^{-6} M recorded at 298 K and of the correspondent mono-charged derivative **3a**, as a representative example for both series of compounds synthesised.
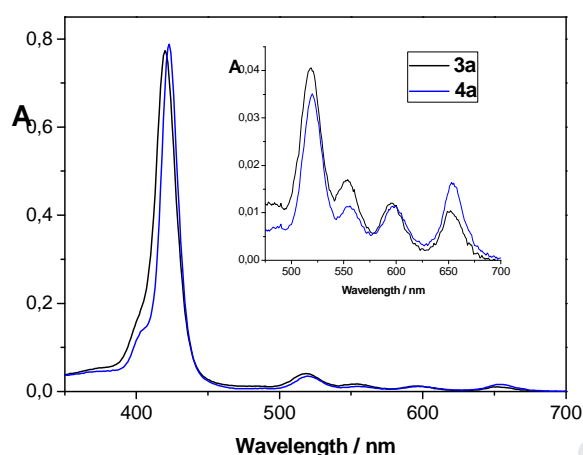
Figure 1. Absorption spectra of compounds **2a** (black line) and **3a** (blue line) at a concentration of 3.0 x 10^{-6} M in DMF at 298 K. The inset shows the absorption at the Q bands region.

In general, the electronic spectra show the typical features of a free-base *meso*-tetraarylporphyrin substituted at a β-pyrrolic position, with a sharp band centred at *ca.* 420 nm (*Soret* band) and four less intense but well-defined bands ranging from 518 to 652 nm (Q bands) due to π–π* transitions.[36-38] When compared with the corresponding neutral derivative, the *Soret* absorption band of the cationic product is red-shifted 3 nm; however, no significant changes were observed in the Q bands zone. In both series, the sharp *Soret* band observed, allowed to conclude that the porphyrinic derivatives are not aggregated in DMF.[38]

One of the most relevant features of a photosensitizer is its aptitude to generate reactive oxygen species (ROS), namely singlet oxygen ($^1O_2$), which is strongly related with the efficiency of the photodynamic process.[39]

The capability of the new synthesised mono-charged porphyrin-imidazole derivatives to generate $^1O_2$ was quantitatively assessed by monitoring the decomposition of 1,3-diphenylisobenzofuran (DPiBF) induced by this cytotoxic species generated during their irradiation with a red light at 630 ± 20 nm.[40] The DPiBF decays obtained after irradiating the conjugates **3a-d** with the red light at an irradiance of 11.0 mW cm^{-2} for 10 min are shown in Figure 2, and were compared with the one induced by 5,10,15,20-tetraphenylporphyrin (**TPP**), selected as reference due to its efficiency to produce oxygen singlet.[41]
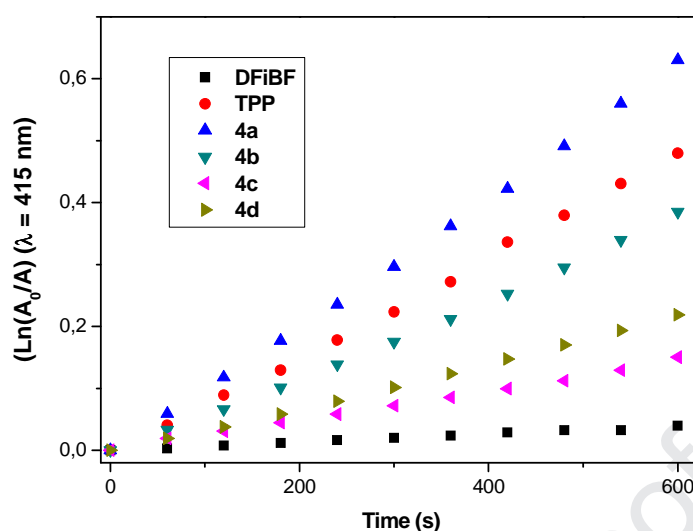
Figure 2. Photodecomposition of DPiBF (50 μM) in the presence and without derivatives **3a-d** and **TPP** at a concentration of 0.5 μM in DMF upon irradiation with red light LEDs (654 nm ± 20 nm) with an irradiance of 11.0 mW cm^{-2}.

The evaluation of the data obtained with the mono-cationic porphyrins **3a-d** confirm that they are all capable to induce the decay of the DPiBF absorption when irradiated with light. It is worth to refer that the absorbance of DPiBF, when irradiated in the absence of a porphyrin derivative, remains almost unchanged.

The most efficient $^1O_2$ producer was derivative **3a** with 0.5 time-fold higher than the reference **TPP**. Compound **3b** present approximately the same ability to generate $^1O_2$ then the reference used in this study. Nevertheless, the two remaining derivatives, **3c** and **3d**, show a noteworthy lower ability to generate $^1O_2$ when compared with the one observed for **TPP**. These results show that the presence of heteroatoms at the substituents into the positions 4 and 5 of the imidazole moiety reduce the capability to produce $^1O_2$. Nevertheless, the ability of these derivatives to generate $^1O_2$, namely compound **3a**, prompt us to evaluate their efficacy as photosensitizers in the inactivation of a Gram-negative bacteria *E. coli.*

2.2 Photodynamic inactivation of *E. coli* using cationic porphyrin-imidazole derivatives 3a-d as PSs and KI

The photodynamic efficiency of the cationic porphyrin-imidazole derivatives **3a-d** was tested against a bioluminescent *E. coli* strain, selected as a bacterial Gram-negative model. Using this bioluminescent approach, the aPDT efficacy of each PS can be checked in real-time, since the viability of the microorganisms is related with its

bioluminescence. In fact, the strong correlation between the colony forming units (CFU) and the bioluminescent signal of the bioluminescent *E. coli* used in this work has already been proved and described.[42]

In order to evaluate the effect of each PS on *E. coli* photoinactivation efficiency, the compounds were tested at different porphyrin concentrations (5.0 and 20.0 µM) in the absence and in the presence of 100 mM of KI. The concentration of this potentiator agent was chosen in agreement with similar studies, which demonstrated that higher concentrations can promote osmotic stress limiting the application of this approach in clinic area.[27] The photodynamic experiments were carried out under irradiation with white light (380–700 nm) at an irradiance of 25 mW.cm^{-2} for 90 min. The results obtained are summarized Fig. 3 and had shown that the inactivation profile of bioluminescent *E. coli* with cationic porphyrin-imidazole derivatives **3a-d** is improved in the KI presence (Figure 3). In all cases, light control, KI control and dark controls did not promote a decrease in the bioluminescence *E. coli* signal, showing that the viability of recombinant bioluminescent *E. coli* was not affected by irradiation, by the presence of PS in the dark and by the presence of KI.

Porphyrin-imidazole derivative **3a** had promoted a decrease of 2.38 $\log_{10}$ RLU (ANOVA, $p<0.05$) and of 3.85 $\log_{10}$ RLU (ANOVA, $p<0.05$) in the bioluminescence of *E. coli* at 5 µM and 20 µM, respectively, after 90 min of irradiation (Figure 3 A). For both concentrations of derivative **3a**, the addition of KI at 100 mM had potentiated the photodynamic effect, causing a decrease of the *E. coli* viability till the detection limit of the method (decrease of 3.90 $\log_{10}$ RLU) after 75 min and 45 min of irradiation, for combination of porphyrin-imidazole derivative **3a** at 5.0 µM + KI and **3a** at 20 µM + KI, respectively.

In what concerns to the results achieved with porphyrin-imidazole **3b** it was possible to observe that this compound is capable to induce a reduction of 1.86 and 3.01 $\log_{10}$ RLU (ANOVA, $p<0.05$) in the viability of *E. coli* after 90 min of irradiation, at 5.0 µM and 20 µM, respectively (Figure 3 B). The combination of this PS with KI had drastically potentiated the photodynamic effect of this PS, since, for both tested concentrations inactivation to the detection limit of the method (decrease of 4.20 $\log_{10}$ RLU) was reached after 15 minutes of irradiation.

Porphyrin-imidazole derivative **3c** revealed to be the less efficient PS in the photoinactivation of bioluminescent *E. coli*, causing a decrease of 0.63 $\log_{10}$ RLU (ANOVA, $p<0.05$) in the viability of the bacterium, after 90 min of irradiation, for both used concentrations (Figure 3C). However, when this compound was used combined with KI the reduction of bioluminescent signal begins after 15 minutes of irradiation and

the inactivation to the detection limit of the method (decrease of *ca.* 4.0 $\log_{10}$ RLU) was reached after 75 minutes of irradiation for 5 µM of **3c** and after 45 minutes of irradiation for 20 µM of **3c**.

The photodynamic profile of porphyrin-imidazole derivative **3d** was also more accentuated when this compound was combined with KI (Figure 3 D). In this case, the inactivation to the detection limit of the method (decrease of 4.0 $\log_{10}$ RLU) was reached after 75 min for combination of derivative **3d** at 5.0 µM + KI and after 30 minutes of irradiation of derivative **3d** at 20 µM + KI. When acting alone, porphyrin-imidazole derivative **3d** caused a decrease of 1.10 and 1.44 $\log_{10}$ RLU (ANOVA, p<0.05) in the viability of *E. coli*, after 90 min of irradiation, for 5.0 and 20 µM, respectively.
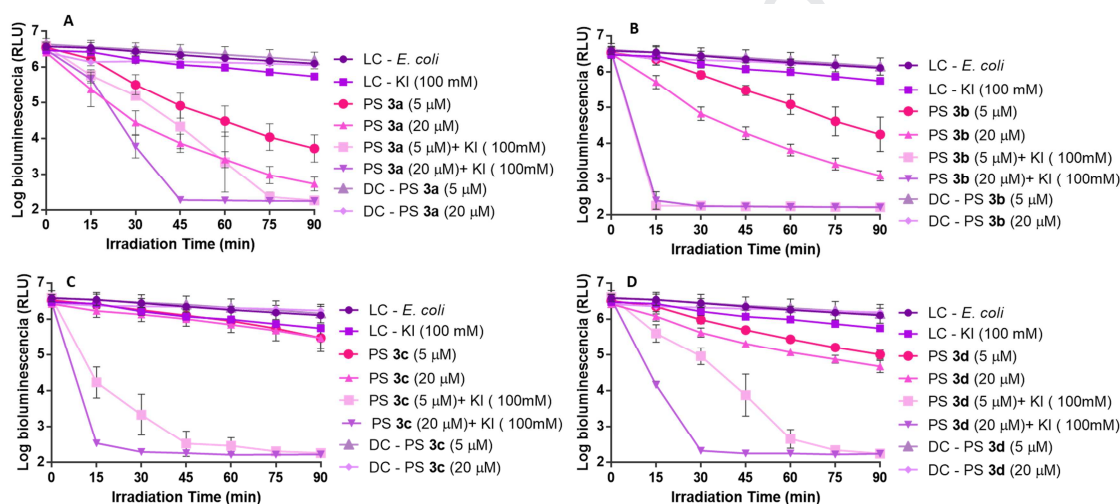

Figure 3. Survival of bioluminescent *E. coli* during aPDT assays in the presence of derivatives **3a** (A), **3b** (B), **3c** (C) and **3d** (D) at 5.0 µM and 20 µM alone and combined with KI at 100 mM. The values are expressed as the three independent experiments with three replicates; error bars signify the SD; DC - dark control; LC - light control.

The photodynamic efficiency of each PS was also correlated with the single oxygen generation. The capability of $^1O_2$ generation of cationic porphyrin-imidazole derivatives **3c** and **3d** was lower than the one achieved for derivatives **3a** and **3b**, which can justify the poor ability to photoinactivate bioluminescent *E. coli* of these PSs when acting alone. Even when combined with KI, these two PSs presented the slower curve of photoinactivation, attaining the detection limit later than the combinations of derivatives **3a** and **3b** with KI. Porphyrin-imidazole derivatives **3a**, when acting alone, revealed to be the most promising

PS achieving higher rates of inactivation of bioluminescent *E. coli*, which is in accordance with the $^1O_2$ generation studies. It is also important to highlight the results achieved with combination of derivative **3b** + KI, where the inactivation curve suffer a sharp decrease in the first 15 min of irradiation. Besides this PS was the second most capable to generate $^1O_2$, the combination with KI highly potentiated its photodynamic effect. Due to the abrupt decrease in the *E. coli* survival rate profile, it is possible to infer that the mechanism of action of the combination porphyrin-imidazole derivative **3b** + KI is probably related to the preferential decomposition of the peroxyiodide into free iodine (I_2/I_3^-).[27, 31]

Cationic porphyrin-imidazole derivatives **3a** and **3b** at 20 µM and combinations of all cationic porphyrin-imidazole derivatives **3a-d** with KI can be considered effective antimicrobial agents for *E. coli* inactivation, according to the American Society for Microbiology, since had promoted a reduction of at least 3 log_{10} in the viability of this bacterium.[43]

3. Experimental section

3.1. General remarks

The starting porphyrin **1** was prepared following a well-established procedure and already reported by our group.[44] Also the oxygen singlet measurements and the biological assays were performed using appropriate procedures already described in the literature.[18, 27] See the supporting information (SI) for a detailed account, as well as, a detailed description of all the equipments used in this study.

3.2. Synthesis

3.2.1. Synthesis of neutral derivatives 2a-d.

A round bottom flask was charged with 2-formyl-5,10,15,20-tetraphenylporphyrin **1** (25 mg, 3.9 x10^{-5} mol) dissolved in a toluene/acetic acid 5:1 mixture (1.5 mL), 1.5 equiv. of the appropriate dione and ammonium acetate (10 equiv.). Then, the reactional mixture was maintained under reflux between 1 to 3 h, until the TLC control showed the full consumption of the starting porphyrin. After this period, the reaction mixture was allowed to cool to room temperature, diluted with CH_2Cl_2 (5 mL), neutralized with an aqueous $NaHCO_3$ solution and extracted with CH_2Cl_2. The organic layer was dried (Na_2SO_4) and the solvent was evaporated in a rotary evaporator. The residue was purified in a

silica gel column chromatography and eluted with CH_2Cl_2 and CH_2Cl_2/MeOH (99:1). The desired products **2a-d** were obtained pure after crystallization from CH_2Cl_2/hexane in yields ranging from 79% to 99%. The porphyrin-imidazole derivatives obtained were fully characterized by adequate spectroscopic techniques.

2-(4,5-Diphenyl-1*H*-imidazol-2-yl)-5,10,15,20-tetraphenylporphyrin, 2a

^{1}H NMR (500 MHz, CDCl₃) = δ 9.26 (1H, s, H-3), 8.86 and 8.84 (2H, AB system, *J* = 4.9 Hz, H-β), 8.82 (1H, d, *J* = 4.8 Hz, H-β), 8.80 (1H, d, *J* = 4.8 Hz, H-β), 8.78 (1H, d, *J* = 4.9 Hz, H-β), 8.74 (1H, d, *J* = 4.9 Hz, H-β), 8.34 (1H, s, H-1´), 8.23-8.20 (6H, m, H-*o*-Ph), 8.16-8.15 (2H, m, H-*o*-Ph), 7.80-7.76 (11H, m, H-*m,p*-Ph), 7.36-7.26 (11H, m, H-*p*-Ph, H-2´,6´, H-3´,5´ and H-4´), -2.62 (2H, s, N-*H*) ppm. ^{13}C NMR (125 MHz, CDCl₃) = δ 143.6, 142.11, 142.06, 141.7, 141.1, 137.3, 135.0, 134.61, 134.6, 133.6, 132.4, 131.0, 130.0, 129.9, 129.4, 129.06, 128.9, 128.8, 128.6, 128.3, 128.0, 127.9, 127.8, 127.7, 127.5, 126.9, 126.74, 126.71, 126.6, 125.2, 120.9, 120.5, 120.4, 120.3 ppm. **MS-ESI(+)**: *m/z* 833.4 [M+H]+. **HRMS-ESI(+)**: *m/z* calculated to $C_{59}H_{41}N_6$ [M+H]+ 833,3421; found, 833,3387. **UV-Vis** (DMF): $λ_{max}$ (log ε) 420 (4.37), 518 (3.29), 552 (2.93), 596 (2.81), 652 (2.76) nm.

2-(4,5-Di(pyridin-2-yl)-1*H*-imidazol-2-yl)-5,10,15,20-tetraphenylporphyrin, 2b

^{1}H NMR (500 MHz, DMSO-d_6) = δ 12.59 (1H, s, N-*H*), 8.99-8.73 (7H, m, H-β), 8.63-8.16 (2H, m, H-6´), 8.27-8.16 (8H, m, H-*o*-Ph and H-3´), 8.03-7.99 (2H, m, H-*o*-Ph), 7.94-7.74 (11H, m, H-*m,p*-Ph and H-4´), 7.30-7.12 (5H, m, H-*m,p*-Ph and H-5´), -2.74 (2H, s, N-*H*) ppm. ^{13}C NMR (125 MHz, DMSO-d_6) = δ 166.1, 156.4, 154.4, 150.3, 149.8, 148.6, 148.5, 148.2, 143.1, 141.4, 141.3, 140.9, 139.7, 138.2, 137.7, 136.3, 136.0, 134.9, 134.3, 134.2, 132.7-130.4 (C-β), 129.5, 128.2, 127.2, 127.1, 126.5, 125.7, 123.3, 122.7, 121.8, 121.6, 120.2, 120.1, 120.0 ppm. **MS-ESI(+)**: *m/z* 835.4 [M+H]+. **HRMS-ESI(+)**: *m/z* calculated to $C_{57}H_{39}N_8$ [M+H]+ 835.3292; found, 835.3323. **UV-Vis** (DMF): $λ_{max}$ (log ε) 419 (4.72), 518 (3.44), 552 (3.04), 595 (2.88), 650 (2.76) nm.

2-(4,5-Di(furan-2-yl)-1*H*-imidazol-2-yl)-5,10,15,20-tetraphenylporphyrin, 2c

^{1}H NMR (500 MHz, DMSO-d_6) = δ 12.26 (1H, s, N-*H*), 8.94-8.88 (3H, m, H-β), 8.83-8.74 (4H, m, H-β), 8.27-8.22 (6H, m, H-*o*-Ph), 8.04 (2H, d, *J* = 7.3 Hz, H-*o*-Ph), 7.85-7.83 (9H, m, H-*m,p*-Ph), 7.75 (2H, d, *J* = 22.7 Hz, H-5´), 7.32 (2H, t, *J* = 7.3 Hz, H-*m*-Ph), 7.26 (1H, t, *J* = 7.3 Hz, H-*p*-Ph), 6.78 (1H, d, *J* = 1.7 Hz, H-3´), 6.69 (1H, d, *J* = 1.7 Hz, H-3´), 6.64-6.59 (2H, m, H-4´), -2.72 (2H, s, N-*H*) ppm. ^{13}C NMR (125 MHz, DMSO-d_6) = δ 149.8, 144.94, 143.2, 142.2, 141.5, 141.4, 141.3, 140.8, 139.5, 135.0, 134.3, 134.1, 132.6-130.4 (C-β), 128.3, 128.2, 127.2, 127.1, 125.9, 121.5, 120.3,

120.2, 120.0, 119.3, 111.7, 111.3, 107.3, 106.4 ppm. **MS-ESI(+)**: *m/z* 813.3 [M+H]⁺. **HRMS-ESI(+)**: *m/z* calculated to $C_{55}H_{37}O_2NO_6$ [M+H]⁺ 813.2973; found, 813.3018. **UV-Vis** (DMF): λ_{max} (log ε) 420 (4.64), 519 (3.49), 552 (3.13), 595 (3.00), 651 (2.94) nm.

2-(1*H*-imidazo[4,5-*f*[1,10]phenanthrolin-2-yl)-5,10,15,20-tetraphenylporphyrin, 2d

¹H NMR (500 MHz, DMSO-d_6) = δ 13.35 (1H, s, N-*H*), 9.09 (1H, s, H-3), 9.06 (2H, dd, *J* = 4.3 and 1.7 Hz, H-6´), 8.93 (2H, s, H-β), 8.88 (1H, d, *J* = 7.3 Hz, H-4´), 8.56 (1H, d, *J* = 7.3 Hz, H-4´), 8.31-8.29 (2H, m, H-*o*-Ph), 8.27-8.23 (4H, m, H-*o*-Ph), 8.09 (2H, d, *J* = 7.3 Hz, H-*o*-Ph), 7.87-7.82 (11H, m, H-*m,p*-Ph and H-5´), 7.01 (2H, t, *J* = 7.4 Hz, H-*m*-Ph), 6.60 (1H, t, *J* = 7.4 Hz, H-*p*-Ph), -2.68 (2H, s, N-*H*) ppm. **¹³C NMR** (125 MHz, DMSO-d_6) = δ 147.7, 147.5, 143.3, 141.3, 141.2, 140.8, 139.7, 135.2, 134.3, 134.2, 133.1-130.4 (C-β), 129.9, 129.4, 128.4, 128.2, 127.2, 127.1, 126.8, 126.3, 125.5, 124.0, 123.3, 123.1, 121.4, 120.5, 120.4, 120.2, 119.1 ppm. **MS-ESI(+)**: *m/z* 833.4 [M+H]⁺. **HRMS-ESI(+)**: *m/z* calculated to $C_{57}H_{37}N_8$ [M+H]⁺ 833.3136; found, 835.3209. **UV-Vis** (DMF): λ_{max} (log ε) 420 (4.41), 519 (3.20), 552 (2.77), 596 (2.62), 651 (2.54) nm.

3.3. Methylation of porphyrin-imidazole derivatives 2a-d: general procedure.

In a sealed tube, the neutral porphyrin-imidazole derivatives **2a-d** (25.0 mg) dissolved in *N,N*-dimethylformamide (1 mL) was treated with an excess of methyl iodide (60 equiv.) and maintained under stirring, at 40 °C for 12 h. After this period, diethyl ether was added and the resulting precipitated was filtered, washed with the same precipitating solvent, and finally dissolved in a mixture of CH_3OH/CH_2Cl_2 (1:9). The solvent mixture was removed under reduced pressure. Compounds **2a-d** were isolated after crystallization in a mixture of CH_2Cl_2/hexane in 81-97%. The compounds obtained were fully characterised by adequate spectroscopic techniques.

2-(4,5-Diphenyl-(1,3-dimethyl)-1*H*-imidazol-3-ium-2-yl)-5,10,15,20-tetraphenylporphyrin iodide, 3a

¹H NMR (500.13 MHz, DMSO-d_6) = δ 9.45 (1H, s, H-3), 9.05 (1H, d, *J* = 4.8 Hz, H-β), 9.01 (1H, d, *J* = 4.8 Hz, H-β), 8.95 (1H, d, *J* = 4.8 Hz, H-β), 8.80 (1H, d, *J* = 4.8 Hz, H-β), 8.76 and 8.73 (2H, AB system, *J* = 4.8 Hz, H-β), 8.37-8.34 (4H, m, H-*o*-Ph), 8.25-8.21 (4H, m, H-*o*-Ph), 7.91-7.79 (12H, m, H-*m,p*-Ph), 7.56-7.50 (6H, m, H-2´,6´and H-4´), 7.41-7.39 (4H, m, H-3´,5´), 3.48 (6H, s, -CH₃), -2.72 (2H, s, N-*H*) ppm. **¹³C NMR** (125 MHz, CDCl₃) = δ 142.5, 140.79, 140.76, 140.6, 139.3, 134.8, 134.4, 134.3, 133.4, 130.8, 130.4, 130.1, 129.2, 129.0, 128.5, 128.4, 127.2, 127.2, 127.1, 125.4, 121.9, 120.8, 120.6, 119.5, 52.8, 34.3 ppm. **MS-ESI(+)**: *m/z* 861.4 [M]⁺. **HRMS-ESI(+)**: *m/z*

calculated to $C_{61}H_{45}N_6^+$ [M]$^+$ 861.3700 found, 861.3723. **UV-Vis** (DMF): λ_{max} (log ε) 423 (5.40), 520 (4.14), 556 (3.70), 597 (3.57), 654 (3.56) nm.

2-(4,5-Di(pyridin-2-yl)-(1,3-dimethyl)-1*H*-imidazol-3-ium-2-yl)-5,10,15,20-tetraphenylporphyrin iodide, 3b

¹H NMR (500.13 MHz, DMSO-d_6) = δ 9.56 (1H, s, H-3), 9.38-931 (1H, m, H-6´´), 9.08-9.02 (2H, m, H-β and H-6´´), 8.97 (1H, d, J = 5.0 Hz, H-β), 8.88-8.81 (2H, m, H-β), 8.76 and 8.73 (2H, AB system, J = 4.8 Hz, H-β), 8.65-8.60 (1H, m, H-3´´), 8.49-8.46 (1H, m, H-3´´), 8.43-8.35 (3H, m, H-*o*-Ph), 8.30-8.18 (3H, m, H-*o*-Ph), 8.11-8.04 (2H, m, H-4´´), 7.94-7.80 (11H, m, H-*m,p*-Ph and H-5´´), 7.73-7.67 (2H, m, H-*m*-Ph), 7.64-7.58 (1H, m, H-*m,p*-Ph), 3.82 (3H, s, -CH$_3$), 3.62 (3H, s, -CH$_3$), -2.71 (2H, s, N-*H*) ppm. **¹³C NMR** (125 MHz, CDCl$_3$) = δ 151.1, 150.9, 150.5, 149.9, 147.0, 146.6, 143.1, 140.8, 140.7, 140.5, 139.6, 139.3, 138.7, 138.4, 137.7, 135.0, 134.9, 134.4, 134.3, 134.2, 134.1, 133.8, 133.4, 131.5, 130.1, 129.5, 129.2, 128.6, 128.4, 127.4, 127.3, 127.2, 126.2, 125.6, 124.8, 124.5, 122.2, 121.7, 121.0, 120.7, 119.3, 47.0, 35.9 ppm. **MS-ESI(+)**: m/z 863.4 [M]$^+$. **HRMS-ESI(+)**: m/z calculated to $C_{59}H_{43}N_8^+$ [M]$^+$. 863.3605; found, 863.3631. **UV-Vis** (DMF): λ_{max} (log ε) 423 (4.53), 520 (3.40), 554 (3.14), 597 (3.11), 653 (3.08) nm.

2-(4,5-Di(furan-2-yl)-(1,3-dimethyl)-1*H*-imidazol-3-ium-2-yl)-5,10,15,20-tetraphenylporphyrin iodide, 3c

¹H NMR (500.13 MHz, DMSO-d_6) = δ 9.50 (1H, s, H-3), 9.05 (1H, d, J = 5.0 Hz, H-β), 9.01 (1H, d, J = 5.0 Hz, H-β), 8.94 (1H, d, J = 5.0 Hz, H-β), 8.79 (1H, d, J = 5.0 Hz, H-β), 8.76 and 8.74 (2H, AB system, J = 4.8 Hz, H-β), 8.36-8.33 (2H, m, H-*o*-Ph), 8.29-8.20 (6H, m, H-*o*-Ph), 8.05 (2H, d, J = 1.7 Hz, H-5´), 7.92-7.81 (9H, m, H-*m,p*-Ph), 7.67-7.64 (3H, m, H-*m,p*-Ph), 7.03 (2H, d, J = 3.4 Hz, H-3´), 6.82 (2H, dd, J = 1.7 and 3.4 Hz, H-4´), 3.59 (6H, s, -CH$_3$), -2.74 (2H, s, N-*H*) ppm. **¹³C NMR** (125 MHz, CDCl$_3$) = δ 163.8, 147.7, 146.2, 144.5, 142.7, 140.8, 140.7, 140.6, 138.9, 138.152, 134.9, 134.7, 134.3, 133.0, 130. 5, 129.0, 128.4, 127.2, 127.2, 126.9, 123.3, 122.0, 120.8, 120.6, 119.4, 115.0, 112.1, 54.9, 35.0 ppm. **MS-ESI(+)**: m/z 841.4 [M]$^+$. **HRMS-ESI(+)**: m/z calculated to $C_{57}H_{41}O_2N_7^+$ [M]$^+$ 841.3286; found, 841.3305. **UV-Vis** (DMF): λ_{max} (log ε) 423 (4.48), 520 (3.14), 557 (2.86), 598 (2.67), 653 (2.66) nm.

2-(1,3-dimethyl)-1*H*-imidazo[4,5-*f*][1,10]phenanthrol-3-ium-2-yl)-5,10,15,20-tetraphenylporphyrin iodide, 3d

¹H NMR (500.13 MHz, DMSO-d$_6$) = δ 8.76 (1H, s, H-3), 9.09 (1H, d, J = 5.0 Hz, H-β), 9.03 (1H, d, J = 5.0 Hz, H-β), 8.93 (1H, d, J = 5.0 Hz, H-β), 8.77-8.73 (3H, m, H-β), 8.40-8.21 (12H, m, H-*o*-Ph, H-4´ and H-6´), 7.97-7.84 (11H, m, H-*m,p*-Ph and H-5´), 7.22-7.12 (2H, m, H-*m*-Ph), 6.75-6.46 (1H, m, H-*p*-Ph), 3.12 (6H, s, -CH$_3$), -2.68 (2H, s, N-*H*) ppm. **¹³C NMR** (125 MHz, CDCl$_3$) = δ 156.3, 152.36, 152.35, 151.6, 149.4,

140.81, 140.75, 140.65, 140.3, 139.8, 139.1, 137.7, 135.2, 134.6, 134.5, 133.5, 133.2, 131.9-129.3 (C-β), 128.7, 128.63, 128.60, 128.4, 127.5, 127.4, 126.9, 126.7, 126.6, 126.2, 125.8, 125.3, 124.6, 124.1, 122.6, 121.7, 121.2, 120.9, 120.4, 119.6, 119.5, 56.3, 38.2 ppm. **MS-ESI(+)**: m/z 861.5 $[M]^+$. **HRMS-ESI(+)**: m/z calculated to $C_{59}H_{41}N_8^+$ $[M]^+$ 861.3449 found, 861.3480. **UV-Vis** (DMF): λ_{max} (log ε) 422 (4.38), 518 (3.13), 552 (2.68), 597 (2.54), 651 (2.46) nm.

3.4 . Antimicrobial Photodynamic Therapy (aPDT) Procedure

E. coli culture was grown overnight and was tenfold diluted in phosphate buffered saline (PBS), pH 7.4, to a final bioluminescence of 10^8 relative light units (RLU) (corresponding to a concentration of $\sim 10^8$ CFU mL^{-1}). The obtained suspension was equally distributed in sterilized beakers. Then, adequate aliquots of each positively charged derivative (**3a-d**) to attain the concentration of 5 μM and 20 μM and 100 mM of KI (total volume was 10 mL per beaker) were added. The samples were remained in the dark for 15 min to favour the porphyrin binding to *E. coli* cells. Light control (LC, containing only the *E. coli* suspension exposed to the same light protocol) and dark control (DC, *E. coli* suspension incubated with each PS at 5 and 20 μM in the absence light) were also carried out simultaneously with the aPDT procedure. Following the incubation period, the samples and LC were exposed to white light irradiation at 2.5 W.m^{-2} under stirring (120 rpm). DC was maintained in the dark during the aPDT procedure. The temperature of each experiment was controlled and kept at 25 °C. Aliquots of 0.8 mL of the samples, LC and DC were collected at time 0 and after 15, 30, 45, 60, 75 and 90 min of aPDT and the bioluminescence signal was assessed in the luminometer. The results were the average of three independent experiments with two replicates.

4. Conclusions

The results presented herein show that porphyrinic derivatives bearing imidazole ring at *beta* position can be prepared in excellent yields through a Radziszewski reaction between 2-formyl-tetraphenylporphyrin and (hetero)aromatic1,2-diones. The neutral derivatives can be cationized in the presence of methyl iodide affording the correspondent mono-charged porphyrin-imidazole derivatives in excellent yields. The photochemical properties of the cationic derivatives show their potential to be used as PSs in photodynamic processes.

The evaluation of the antimicrobial properties against bioluminescent *E. coli* as a Gram-negative bacterial model showed that these mono-charged porphyrin-imidazole derivatives **3a-d** efficiently photoinactivate this bacterium and the efficiency of the photoinactivation profile is highly improved in the presence of KI.

References

[1] Davies J, Davies D. Origins and evolution of antibiotic resistance. Microbiol Mol Biol Rev. 2010;74(3):417-33.

[2] Marciel L, Teles L, Moreira B, Pacheco M, Lourenco LMO, Neves M, et al. An effective and potentially safe blood disinfection protocol using tetrapyrrolic photosensitizers. Future Med Chem. 2017;9(4):365-79.

[3] Kashef N, Huang Y-Y, Hamblin MR. Advances in antimicrobial photodynamic inactivation at the nanoscale. Nanophotonics. 2017;6(5):853-79.

[4] Cieplik F, Deng D, Crielaard W, Buchalla W, Hellwig E, Al-Ahmad A, et al. Antimicrobial photodynamic therapy – what we know and what we don't. Crit Rev Microbiol. 2018;44(5):571-89.

[5] Hamblin MR, Hasan T. Photodynamic therapy: a new antimicrobial approach to infectious disease? Photochem Photobiol Sci. 2004;3(5):436-50.

[6] Costa L, Tomé JPC, Neves MGPMS, Tomé AC, Cavaleiro JAS, Faustino MAF, et al. Evaluation of resistance development and viability recovery by a non-enveloped virus after repeated cycles of aPDT. Antiviral Res. 2011;91(3):278-82.

[7] Almeida A, Faustino MA, Tomé JP. Photodynamic inactivation of bacteria: finding the effective targets. Future Med Chem. 2015;7(10):1221-4.

[8] Wainwright M. Photodynamic antimicrobial chemotherapy (PACT). J Antimicrob Chemother. 1998;42(1):13-28.

[9] Alves E, Costa L, Carvalho CMB, Tomé JPC, Faustino MA, Neves MGPMS, et al. Charge effect on the photoinactivation of Gram-negative and Gram-positive bacteria by cationic meso-substituted porphyrins. BMC Microbiol. 2009;9:70-.

[10] Sagrillo FS, Dias C, Gomes ATPC, Faustino MAF, Almeida A, Gonçalves de Souza A, et al. Synthesis and photodynamic effects of new porphyrin/4-oxoquinoline derivatives in the inactivation of S. aureus. Photochem Photobiol Sci. 2019;18(8):1910-22.

[11] Almeida A, Cunha A, Faustino MAF, Tomé AC, Neves MGPMS. Chapter 5 Porphyrins as Antimicrobial Photosensitizing Agents. Photodynamic Inactivation of Microbial Pathogens: Medical and Environmental Applications: The Royal Society of Chemistry; 2011. p. 83-160.

[12] Garcia-Sampedro A, Tabero A, Mahamed I, Acedo P. Multimodal use of the porphyrin TMPyP: From cancer therapy to antimicrobial applications. J Porphyrins Phthalocyanines. 2019;23(01n02):11-27.

[13] Gomes ATPC, Cunha AC, Domingues MdRM, Neves MGPMS, Tomé AC, Silva AMS, et al. Synthesis and characterization of new porphyrin/4-quinolone conjugates. Tetrahedron. 2011;67(38):7336-42.

[14] Bellina F, Cauteruccio S, Rossi R. Synthesis and biological activity of vicinal diaryl-substituted 1H-imidazoles. Tetrahedron. 2007;63(22):4571-624.

[15] Batista RMF, Costa SPG, Belsley M, Raposo MMM. Synthesis and optical properties of novel, thermally stable phenanthrolines bearing an arylthienyl-imidazo conjugation pathway. Dyes Pigments. 2009;80(3):329-36.

[16] Ferreira RCM, Costa SPG, Gonçalves H, Belsley M, Raposo MMM. Fluorescent phenanthroimidazoles functionalized with heterocyclic spacers: synthesis, optical chemosensory ability and two-photon absorption (TPA) properties. New J Chem. 2017;41(21):12866-78.

[17] Okda HE, El Sayed S, Otri I, Ferreira RCM, Costa SPG, Raposo MMM, et al. A simple and easy-to-prepare imidazole-based probe for the selective chromo-fluorogenic recognition of biothiols and Cu(II) in aqueous environments. Dyes Pigments. 2019;162:303-8.

[18] Moura NMM, Esteves M, Vieira C, Rocha GMSRO, Faustino MAF, Almeida A, et al. Novel β-functionalized mono-charged porphyrinic derivatives: Synthesis and photoinactivation of Escherichia coli. Dyes Pigments. 2019;160:361-71.

[19] Kubota R, Takabe T, Arima K, Taniguchi H, Asayama S, Kawakami H. New class of artificial enzyme composed of Mn-porphyrin, imidazole, and cucurbit[10]uril toward use as a therapeutic antioxidant. J Mater Chem B. 2018;6(43):7050-9.

[20] Jinks MA, Sun H, Hunter CA. Measurement of supramolecular effective molarities for intramolecular H-bonds in zinc porphyrin–imidazole complexes. Org Biomol Chem. 2014;12(9):1440-7.

[21] Mahmoudi L, Mohajer D, Kissner R, Koppenol WH. Water increases rates of epoxidation by Mn(iii)porphyrins/imidazole/IO4– in CH2Cl2. Analogy with peroxidase and chlorite dismutase. Dalton Trans. 2011;40(34):8695-700.

[22] Liao M-S, Huang M-J, Watts JD. Iron Porphyrins with Different Imidazole Ligands. A Theoretical Comparative Study. J Phys Chem A. 2010;114(35):9554-69.

[23] Warren JJ, Mayer JM. Hydrogen Atom Transfer Reactions of Iron–Porphyrin–Imidazole Complexes as Models for Histidine-Ligated Heme Reactivity. J Am Chem Soc. 2008;130(9):2774-6.

[24] Marczak R, Sgobba V, Kutner W, Gadde S, D'Souza F, Guldi DM. Langmuir–Blodgett Films of a Cationic Zinc Porphyrin–Imidazole-Functionalized Fullerene Dyad: Formation and Photoelectrochemical Studies. Langmuir. 2007;23(4):1917-23.

[25] Seng V, Wang X, Ali R, Fang W, Charles-Pierre F, Bhagan S, et al. Synthesis of imidazole and imidazolium porphyrins. J Heterocycl Chem. 2006;43(4):1077-81.

[26] Sharma S, Nath M. An efficient synthetic approach to novel nickel(II) 2-benzazolo-5,10,15,20-tetraphenylporphyrins. J Heterocycl Chem. 2012;49(1):88-92.

[27] Vieira C, Gomes ATPC, Mesquita MQ, Moura NMM, Neves MGPMS, Faustino MAF, et al. An Insight Into the Potentiation Effect of Potassium Iodide on aPDT Efficacy. Front Microbiol. 2018;9(2665).

[28] Vecchio D, Gupta A, Huang L, Landi G, Avci P, Rodas A, et al. Bacterial Photodynamic Inactivation Mediated by Methylene Blue and Red Light Is Enhanced by Synergistic Effect of Potassium Iodide. Antimicrob Agents Chemother. 2015;59(9):5203-12.

[29] Zhang YS, Dai TH, Wang M, Vecchio D, Chiang LY, Hamblin MR. Potentiation of antimicrobial photodynamic inactivation mediated by a cationic fullerene by added iodide: in vitro and in vivo studies. Nanomed. 2015;10(4):603-14.

[30] Freire F, Ferraresi C, Jorge AOC, Hamblin MR. Photodynamic therapy of oral Candida infection in a mouse model. J Photochem Photobiol, B. 2016;159:161-8.

[31] Hamblin MR. Potentiation of antimicrobial photodynamic inactivation by inorganic salts. Expert Rev Anti-Infective Ther. 2017;15(11):1059-69.

[32] Reynoso E, Quiroga ED, Agazzi ML, Ballatore MB, Bertolotti SG, Durantini EN. Photodynamic inactivation of microorganisms sensitized by cationic BODIPY derivatives potentiated by potassium iodide. Photochem Photobiol Sci. 2017;16(10):1524-36.

[33] Huang LY, Szewczyk G, Sarna T, Hamblin MR. Potassium Iodide Potentiates Broad-Spectrum Antimicrobial Photodynamic Inactivation Using Photofrin. Acs Infect Dis. 2017;3(4):320-8.

[34] Huang L, Bhayana B, Xuan W, Sanchez RP, McCulloch BJ, Lalwani S, et al. Comparison of two functionalized fullerenes for antimicrobial photodynamic inactivation: Potentiation by potassium iodide and photochemical mechanisms. J Photochem Photobiol, B. 2018;186:197-206.

[35] Vieira C, Santos A, Mesquita MQ, Gomes ATPC, Neves MGPMS, Faustino MAF, et al. Advances in aPDT based on the combination of a porphyrinic formulation with potassium iodide: Effectiveness on bacteria and fungi planktonic/biofilm forms and viruses. J Porphyrins Phthalocyanines. 2019;23(04n05):534-45.

[36] D'Aléo A, Gachet D, Heresanu V, Giorgi M, Fages F. Efficient NIR-Light Emission from Solid-State Complexes of Boron Difluoride with 2′-Hydroxychalcone Derivatives. Chem Eur J. 2012;18(40):12764-72.

[37] Hashimoto T, Choe Y-K, Nakano H, Hirao K. Theoretical Study of the Q and B Bands of Free-Base, Magnesium, and Zinc Porphyrins, and Their Derivatives. J Phys Chem A. 1999;103(12):1894-904.

[38] Maximiano RV, Piovesan E, Zílio SC, Machado AEH, de Paula R, Cavaleiro JAS, et al. Excited-state absorption investigation of a cationic porphyrin derivative. J Photochem Photobiol, A. 2010;214(2):115-20.

[39] Di Mascio P, Martinez GR, Miyamoto S, Ronsein GE, Medeiros MHG, Cadet J. Singlet Molecular Oxygen Reactions with Nucleic Acids, Lipids, and Proteins. Chem Rev. 2019;119(3):2043-86.

[40] Spiller W, Kliesch H, WÖHrle D, Hackbarth S, RÖDer B, Schnurpfeil G. Singlet Oxygen Quantum Yields of Different Photosensitizers in Polar Solvents and Micellar Solutions. J Porphyrins Phthalocyanines. 1998;02(02):145-58.

[41] Zenkevich E, Sagun E, Knyukshto V, Shulga A, Mironov A, Efremova O, et al. Photophysical and photochemical properties of potential porphyrin and chlorin photosensitizers for PDT. J Photochem Photobiol, B. 1996;33(2):171-80.

[42] Alves E, Carvalho CMB, Tomé JPC, Faustino MAF, Neves MGPMS, Tomé AC, et al. Photodynamic inactivation of recombinant bioluminescent Escherichia coli by cationic porphyrins under artificial and solar irradiation. J Ind Microbiol Biotechnol. 2008;35(11):1447.

[43] Pankey GA, Sabath LD. Clinical Relevance of Bacteriostatic versus Bactericidal Mechanisms of Action in the Treatment of Gram-Positive Bacterial Infections. Clin Infect Dis. 2004;38(6):864-70.

[44] Moura NMM, Faustino MAF, Neves M, Duarte AC, Cavaleiro JAS. Vilsmeier-Haack formylation of Cu(II) and Ni(II) porphyrin complexes under microwaves irradiation. J Porphyrins Phthalocyanines. 2011;15(7-8):652-8.

An insight into the synthesis of cationic porphyrin-imidazole derivatives and their photodynamic inactivation efficiency against *Escherichia coli*

Xavier Moreira,[a] Patrícia Santos,[b] M. Amparo F. Faustino,[a] M. Manuela M. Raposo,[c] Susana P. G. Costa,[c] Nuno M. M. Moura,[a,*] Ana T. P. C. Gomes,[b,*] Adelaide Almeida,[b] M. G. P. M. S. Neves[a,*]

[a] *QOPNA & LAQV-REQUIMTE, Department of Chemistry, University of Aveiro, 3810-193 Aveiro, Portugal. E-mail:* nmoura@ua.pt; gneves@ua.pt

[b] *CESAM and Department of Biology, University of Aveiro, 3810-193 Aveiro, Portugal. E-mail:* ana.peixoto@ua.pt;

[c] *Centro de Química, Universidade do Minho, Campus de Gualtar, 4710-057 Braga, Portugal.*

Highlights

- β-functionalized porphyrinic derivatives bearing imidazole were prepared by a Radziszewski reaction

- The alkylation/cationization of the imidazole ring was efficiently achieved affording the mono-charged β-porphyrinic derivatives

- All the new derivatives are able to generate singlet oxygen

- The cationic porphyrin-imidazole showed the ability to be used as photosensitizer in the photoinactivation of bioluminescent *E. coli*

- The efficiency of the photosensitizer is meaningfully improved in the presence of KI

Authors contributions

Investigation – X. Moreira and N. M. M. Moura (Porphyrin-imidazole derivatives synthesis and characterization); S. P. G. Costa (1,2-Diones preparation); P. Santos and A. T. P. C. Gomes (Biological assays)

Supervision – A. Alemida, M. M M. Raposo and M. G. P. M. S. Neves;

Validation – M. M. M. Raposo, M. A. F. Faustino

Writing – original draft, N. M. M. Moura and A. T. P. C. Gomes

Writing - review and editing, N. M. M. Moura, A.T. P. C. Gomes, M. M. Raposo, S. P. G. Costa, A. Almeida and M. G. P. M. S. Neves.

Declaration of interests

☒ The authors declare that they have no known competing financial interests or personal relationships that could have appeared to influence the work reported in this paper.

☐The authors declare the following financial interests/personal relationships which may be considered as potential competing interests: